“SYNTHESIS AND CHARACTERISATION OF $Co_{0.5}Ni_{0.5}Fe_2O_4$ BY COMBUSTION METHOD AND TO STUDY THE EFFECT OF SINTERING TEMPERATURE ON ITS SOLID STATE PROPERTIES”

“SYNTHESIS AND CHARACTERISATION OF $Co_{0.5}Ni_{0.5}Fe_2O_4$ BY COMBUSTION METHOD AND TO STUDY THE EFFECT OF SINTERING TEMPERATURE ON ITS SOLID STATE PROPERTIES”

A PROJECT SUBMITTED
BY

MISS VAIBHAVI SHANKAR NAIK

TO THE

SCHOOL OF CHEMICAL SCIENCES
GOA UNIVERISTY
GOA – 403206
APRIL 2020

STATEMENT

I hereby declare that the matter presented in this dissertation entitled, “Synthesis and characterisation of $Co_{0.5}Ni_{0.5}Fe_2O_4$ by combustion method and to study the effect of sintering temperature on its solid state properties” is based on the results of investigations carried out by me in the School of Chemical Sciences, Goa University, Goa under the supervision of Dr. V. M. S. Verenkar and the same has not been submitted elsewhere for the award of a degree or diploma.

Miss Vaibhavi Naik
CH-18-055
School of Chemical Sciences **Date:**

CERTIFICATE

This is to certify that the dissertation entitled “Synthesis and characterisation of $Co_{0.5}Ni_{0.5}Fe_2O_4$ by combustion method and to study the effect of sintering temperature on its solid state properties” is bonafide work carried out by Ms. Vaibhavi Shankar Naik under my supervision is partial fulfilment of the requirement for the award of the degree of Master of Science in Chemistry at the School of Chemical Sciences, Goa University, Goa.

Dr. V.M.S. Verenkar
Guiding Teacher
School of Chemical Sciences
Goa University, Goa

CERTIFCATE

This is to certify that the dissertation entitled, “Synthesis and characterisation of $Co_{0.5}Ni_{0.5}Fe_2O_4$ by combustion method and to study the effect of sintering temperature on its solid state properties” is bonafide work carried out by Ms. Vaibhavi Shankar Naik under the supervision of Dr. V.M.S. Verenkar for the award of the degree of Master of Science in Chemistry at the School of Chemical Sciences, Goa University, Goa.

Prof. V.S. Nadkarni
Dean,
School Chemical Sciences
Goa University, Goa

ACKNOWLEDGEMENT

First of all I am very thankful to the ALMIGHT for being with me all the time. I would like to take this opportunity to express my sincere gratitude to all who helped me in working out my project.

My Sincere ‘THANK YOU’ to my Project guide Dr. V.M.S Verenker, for his constant encouragement, energetic interest and immense motivation which has been the source of inspiration for me.

I also extend my deep gratitude to our Dean of School Of Chemical Sciences Prof. V.S Nadkarni and my Teachers for providing with all the necessary facilities.

I express my sincere thanks to research scholars from School of Chemical Sciences Ms. Prajyoti Gauns Dessai, Ms. Mangala Sawal , Mr. Pratik Asogekar for guiding and helping in doing project work. I am thankful to Ms. Mangala Sawal for helping me out in recording IR data.

I also wish to offer my humble gratitude to Mr. Girish Prabhu , NIO Dona-Paula for helping me with XRD of the samples. I would also like to thank USIC, Goa University for recording SEM images of samples.

A word of thanks to Mr. Deepak Chari and laboratory attendant for providing us with all the help needed.

I would also like to thanks my friends Ms Riddhi Goltekar and Karishma Naik for helping me in my project work.

Last but not the least I would like to extend my deep gratitude to my parents, for unceasing support and encouragement.

CONTENT

CHAPTER-I

INTRODUCTION

1. INTRODUCTION

The wide interest in ferrite nanoparticles is due to their unique and unusual chemical and physical properties with their high surface activities. A key factor for improving the properties of these particles due to their miniature size lies in enhancing the fraction of their surface atoms. It is useful in many applications such as recording media, microwave devices, pigments, high frequency cores, high-density magnetic information storage, absorbents, and sensors [1-2]. Indeed, ferrite based materials show a unique structural, morphological, chemical, mechanical, electric, and magnetic properties [4-21]. Ferrite based materials can be prepared using different methods [7]. The combustion process is among the important method for preparing of different ferrites [8–11]. Both doping and substitution processes resulted in a progressive change in the magnetic properties of ferrites depending on micro-structure and particle size of the as synthesized ferrites [12–14]. The structural and magnetic properties of nanocrystalline ferrites are affected by a variety of factors including processing conditions, sintering temperature, precursor atmosphere, chemical composition, cation distribution in the tetrahedral (A) and octahedral [B] sites, grain size, voids, surface layers, and doping [18].

As important members in the family of spinel ferrites, nickel ferrite ($NiFe_2O_4$) and cobalt ferrite ($CoFe_2O_4$) materials have been accepted as the promising candidates for a wide variety of applications including ferrofluids, catalysts, magnetic drug delivery and magnetic high-density information storage [20–23].]. $Ni_{1-x}Co_xFe_2O_4$ nano particles belong to spinel type lattice with space group Fd3m [18].

Cobalt ferrite is a well-known hard magnetic material with relatively high coercivity and saturation magnetization, as well as great physical and chemical stabilities [9–11]. So, cobalt ferrite is suitable for many practical applications such as audio/video tapes, high density digital recording disks and so on [12]. Nano-crystalline $CoFe_2O_4$ system with an average grain size of about 50 nm were successfully synthesized using a combustion method employing different ratios of fuel to cations up to 2.67 [12]. The structure, surface activity, selectivity and magnetic properties of cobalt ferrite were altered by changing the fuel/oxidiser ratio. A fuel/oxidiser ratio optimization led to the formation of $CoFe_2O_4$ having a high activity (49%) and magnetization (77.54 emu/g) [12].

Nickel ferrite is a soft material with low coercivity and saturation magnetization. So, nickel ferrite has many applications in electronic devices, such as inductors and transformer cores [13]. Ni is a ferromagnetic metal which magnetizes easily even at room temperature, and hence, to increase the magnetization value of $CoFe_2O_4$, an attempt has been made to substitute the divalent Ni into $CoFe_2O_4$ lattice [25]. A series of Ni substituted $CoFe_2O_4$ nanoparticles using the aerosol chemical route. They found that as the concentration of Ni^{2+} into the $CoFe_2O_4$ matrix increases, the particle size decreases, and thus, the saturation magnetization decreases. They also exhibit ferrimagnetism, originating from the magnetic moment of anti-parallel spins between Fe^{3+} ions at tetrahedral sites and Co^{2+} or Ni^{2+} ions at octahedral sites [26].

Ferrites, as conventional EM wave absorbing materials, have been extensively studied because of their strong magnetism and high electric resistivity [27] and some of them have been already applied in both military and civil fields.

Recently, electrospinning has been extensively explored as a simple and effective method to fabricate various ultrathin inorganic [28-29] fibres with the diameter ranging from tens of nanometres to several micrometres. Ferrites, as conventional EM wave absorbing materials, have been extensively studied because of their strong magnetism and high electric resistivity [12] and some of them have been already applied in both military and civil fields. [,18]. Co–Ni ferrites with excellent electromagnetic properties are important electronic materials and used in electronic devices for high-frequency applications in the telecommunication field [30]. The ferromagnetic behaviour of cobalt ferrite nanoparticles are observed when they crystallize in the inverse spinel structure with tetrahedral A-site coordination, $Co1-\delta Fe\delta O4$, and octahedral B-site coordination $Co\delta Fe1-\delta O4$, where δ represents the degree of inversion $\delta = 1$ for the inverse spinel structure and $\delta = 0$ for the normal spinel structure [31-35].

1.1 Classification of Ferrites:

Ferrites are classified into four crystal categories

1.1.1 Garnet

The general chemical formula for the unit cell of a pure iron garnet have eight formula units of $M_3Fe_5O_{12}$ where M is the trivalent rare earth ion (Y, Gd, Dy). The metal ion occupy the dodecahedral sites (called C sites), where they are surrounded by eight oxygen ion ,the Fe^{+3} ions are distributed over the tetrahedral and octahedral sites in the ratio 3:2.

1.1.2 Spinel Ferrites

In spinel ferrites cations are distributed at tetrahedral A and octahedral B site depending upon their ionic radii, electronic configuration, and the electrostatic energy of the lattice. On the occupancy of the cations at tetrahedral A and octahedral B sites, the Spinel ferrites are classified as inverse, normal and random spinel ferrites. Spinel ferrites have chemical formula MFe_2O_4.

There are three types of Spinel Ferrites:

a) **Normal Spinel Ferrites** : In these types of Ferrites the divalent metal ion are totally occupied at tetrahedral A site and trivalent ferric ions are totally occupied at octahedral B site. This types of ferrites is represented by MFe_2O_4 and can be written as $[M]^A[Fe_2]^BO_4$. Example of such type of ferrite is $ZnFe_2O_4$.

b) **Inverse spinel Ferrites** : In these types of Ferrites the divalent metal ion are totally occupies octahedral B site where as the trivalent ferric ion equally occupy tetrahedral A and octahedral sites B. This type of ferrite is represented as $[Fe]^A\ [MFe]^BO_4$. The examples of this inverse spinel ferrite is Cobalt ferrite and Nickel Ferrite.

c) **Random Ferrites:** when divalent metal ion and trivalent ferric ions occupy both tetrahedral and octahedral sites. This distribution of spinel ferrites can be represented as $[M_{1-x}Fe_x][Fe_{2-x}M_x]O_4$ where x is distribution parameter and can very between o to 1. Magnesium and Copper ferrites are example of random ferrites.

1.1.3 Magneto plumbite

They are represented by chemical formula $MFe_{12}O_{19}$ having hexagonal structure , where M is a divalent ion such as Ba^{+2}, Sr^{+2}, Pb^{+2} with large ionic radius. Crystal structure, like barium and strontium ferrites $BaFe_{12}O_{19}$ ($BaO:6Fe_2O_3$) and $SrFe_{12}O_{19}$ ($SrO:6Fe_2O_3$)

1.1.4 Ortho Ferrites

They crystallize in a distorted Perovskite structure with an orthorhombic unit cell. They have a general formula of ABO_3 with a cubic structure. A site ions are on the corners of the lattice is a large trivalent or divalent metal ion, such as earth ion. B site ion on the centre of the lattice can be 3d, 4d and 5d transition metal ion. A large number of metallic elements are stable in the Perovskites structure. Perovskites exhibit sub metallic to metallic properties. They are colourless and brittle with lustre.

1.2 Classification of Magnetic material

a) Diamagnetism

These substances do not contain any unpaired electron. The small circulating current produces a magnetic field which opposes the external magnetic field hence these are repelled by the magnetic field. In absence of the magnetic field the atoms of the diamagnetic material have known magnetic moment. The value of susceptibility for such material is independent of temperature and is negative. Bismuth, copper , quartz are example of the diamagnetic material.

b) Paramagnetic materials

In these materials there is no interaction between individual atoms. Each atom has magnetic moment which is randomly oriented as a result of thermal agitation. The substance obeys Curie or Curie Weiss law. On application of external field there is slight alignment of these moment which produces low magnetisation in the direction of applied field. The susceptibility of such material is positive.

c) Ferromagnetic materials

In these materials electron spin of each of the atom couple together to form resultant unit cell magnetic moment. Ferromagnetism is possible only when the atoms are arranged in a lattice and the atomic magnetic moments can interact to align parallel to each other. In these materials spontaneous magnetisation takes place only below ferromagnetic Curie temperature Tc and above Tc they behave as paramagnetic material. Magnetic susceptibility is positive.

d) Antiferromagnetic materials

In these materials there is equal number of two alignments so that in the absence of magnetic field there is no resultant magnetization. For these materials susceptibility is temperature dependent. Above Neel’s temperature antiferromagnetic materials behave as paramagnetic materials.

e) Ferrimagnetic materials

These materials showing ferrimagnetism generally have ion on two sets of lattice sets. These ions have opposed spin arrangement. But unlike antiferromagnetic material they do not cancel each other and therefore there is resultant permanent magnetic moment. Iron oxide is the best example of ferromagnetic materials.

1.3 Preparation of Ferrites

There are several techniques for the preparation of ferrites. They are divided into two categories.

a) Solid state method

This method includes conventional ceramic method and is also called heat and beat method. But the disadvantage of this method is that it does not give homogenous product and the method is very sluggish. Particle size is very high, in micrometre range.

b) Solution method

This method includes co-precipitation, Precursor method, Combustion method, Sol gel method, etc. These methods gives homogenous product and the particle size formed is in nanoscale range hence more preferred over solid state method.

1.4 Application of Ferrites

- The magnetostrictive property is used in transducer application.
- Ferrites with narrow hysteresis loop are obvious choices for transformer and inductor core at radio frequencies.
- Ferrites of a type known as square-loop ferrites can be magnetized in either of two directions by an electric current. This property makes them useful in the memory cores of digital computers,
- Hard ferrites are used in permanent magnet. Barium hard ferrites are used as focusing magnets for TV tubes.
- The soft ferrites are useful at high frequencies with high resistivity, high permeability
- The ferrites with rectangular hysteresis loop are used in data storage and are also useful as computer memory devices.
- Spinel ferrites and garnets are used in microwave applications.
- In medical field these magnetic nanoparticles of ferrites are used for drug targeting and hyperthermia, separation and magnetic resonance imaging.
- Ferrite nanoparticles are used in treating polluted waste water from industry.

1.5 Literature Review

Mathew George et al. [30], studied properties o32f sol–gel synthesized $CoFe_2O_4$ powders, deviation from Maxwell–Wagner theory and evidence of surface polarization effects. Fine particles of cobalt ferrite were synthesized by the sol–gel method. Subsequent heat treatment at different temperatures yielded cobalt ferrites having different grain sizes. X-ray diffraction studies were carried out to elucidate the structure of all the samples. Dielectric permittivity and ac conductivity of all the samples were evaluated as a function of frequency, temperature and grain size. The variation of permittivity and ac conductivity with frequency reveals that the dispersion is due to Maxwell–Wagner type interfacial polarization in general, with a noted variation from the expected behaviour for the cold synthesized samples. R C Kambale, P A Shaikh, C H Bhosale, K Y Rajpure and Y D Kolekar[31] investigated dielectric properties and complex impedance spectroscopy studies of mixed Ni–Co ferrites. Ferrites with general formula $Ni_{(1-x)}Co_xFe_2O_4$ (where $x = 0.0, 0.2, 0.4, 0.6$ and 0.8) were prepared by the conventional double sintering ceramic method. The microstructural features were observed by scanning electron microscopy. An infrared spectroscopy study indicates the presence of tetrahedral and octahedral group complexes, respectively, within the spinel phase. Increase of the dielectric permittivity is observed with increase of the cobalt concentration in the nickel ferrite matrix. The results of complex impedance measurements show that as the cobalt concentration increases, the total impedances (*Z*_ and *Z*__) decrease. AC conductivity measurements suggest that the conduction in the present system may be due to the polaron hopping mechanism.

Jun Xiang, Yanqiu Chu, Xionghui Zhang and Xiangqian Shen [32] studied magnetic and microwave absorption properties of electrospun $Co_{0.5}Ni_{0.5}Fe_2O_4$ nanofibers with 70–100 nm in diameter prepared via electrospinning and calcination process. They reported that the saturation magnetization gradually enhances from 37.5 to 66.2 emu/g with increasing calcination temperature from 450 to 800 °C, while the corresponding coercivity increases initially, achieving a maximum value of 78.3 kA/m at 600 °C and then decreases with further increase in calcination temperature due to the transformation of magnetic structure from single-domain to multi-domain. Lei Zhang, Chunsheng Shi, Kyong Yop Rhee and Naiqin Zhao [33] carried out study on properties of $Co_{0.5}Ni_{0.5}Fe_2O_4$/carbon nanotubes/polyimide nanocomposites for microwave absorption. Multi-walled carbon nanotubes (MWNTs) were surface modified by Ar plasma and $Co_{0.5}Ni_{0.5}Fe_2O_4$ nanoparticles were doped onto the surface of the MWNTs by a chemical co-precipitation method. $Co_{0.5}Ni_{0.5}Fe_2O_4$/MWNTs powders were then added to polyimide to prepare nanocomposites for microwave absorption. High-temperature microwave absorbing materials are of great interest due to their ability to withstand high temperatures. L. R. Gonsalves and V. M. S. Verenkar [34] investigated synthesis and characterization of nanosize nickel-doped cobalt ferrite obtained by precursor combustion method. Nanoparticles of the spinel ferrite, $Co_{1-x}Ni_xFe_2O_4$ (x = 0, 0.2, 0.3) have been synthesized by the precursor combustion technique. Novel precursors of metal fumarato-hydrazinate have been employed to yield the nanosized spinel ferrite. The thermal decomposition pattern of the precursors has been studied by isothermal thermogravimetric and differential thermal analysis. In order to fix the chemical composition, the precursors have been characterized by FTIR and chemical analysis and their chemical composition has been fixed accordingly. The Curie temperature of the “as-prepared” ferrites was determined by alternating current susceptibility measurements.

N.M. Deraz et al. [35] studied the processing and characterization of nano-magnetic $Co_{0.5}Ni_{0.5}Fe_2O_4$ system. In their study, the XRD and IR analyses enabled them to determine the functional group and structural parameters of $Co_{0.5}Ni_{0.5}Fe_2O_4$. The EDX measurements showed the concentrations of O, Ni, Fe, and Co species involved in $Co_{0.5}Ni_{0.5}Fe_2O_4$ specimen from the uppermost surface to the bulk layers. The magnetization and coercivity of the as synthesized composite were 77 emu/g and 128 Oe, respectively. Kishwar khan [36] studied microwave absorption properties of radar absorbing nanosized Cobalt ferrites for high frequency applications. Radar absorbing materials, nickel-cobalt ferrites (NCF) of general formula $Ni_{(1-x)}Co_{(x)}Fe_2O_4$ ($0.0 \le x \le 0.5$) were synthesized by the co-precipitation route. The x-ray diffraction studies confirmed that all the samples exhibit the single-phase cubic spinel structure. The structural morphology of the prepared samples was carried out using SEM. SEM images indicated that the final product consists of nano rods, and their chemical compositions were measured using the energy dispersive spectroscopy (EDS) technique. The infrared spectra are measured in the frequency range 700–350 cm^{-1}. Furthermore, the influence of Co on the magnetic and microwave absorbance characteristics by using VSM and network analyser of $Ni_{(1-x)}Co_{(x)}Fe_2O_4$ ($0.0 \le x \le 0.5$ nanoparticles, has been investigated, respectively, in detail. The results show that the low loss Ni substituted Co ferrites is an excellent magnetic material for VHF (very high frequency; 30–300 MHz) miniature antenna applications.

S. Bakhshayesh and H. Dehghani [37] studied synthesis, magnetic properties and the use as magnetic adsorbent for removing lead(II) ion of nickel and cobalt ferrites nanoparticles. In their study nano-sized nickel ferrite ($NiFe_2O_4$) and cobalt ferri42te particles ($CoFe_2O_4$) were successfully synthesized using a hydrothermal method. The techniques of X-ray diffraction, scanning electron microscope, Fourier transform infrared spectrometer, energy dispersive X-ray spectroscopy, vibrating sample magnetometer and transmission electron microscope have been used to characterize and study the as-synthesized $NiFe_2O_4$ and $CoFe_2O_4$ products. The results showed that the average size of the nickel and cobalt ferrite nanoparticles is smaller than 10 and 100 nm, respectively. The results of magnetic measurement showed that the synthesized $NiFe_2O_4$ and $CoFe_2O_4$ nanoparticles were superparamagnetic and soft ferromagnetic materials, respectively. The study of adsorption behaviour showed that these nanoparticles can act as a good adsorbent for removing Pb^{2+}. Hafiz M.I. Abdallah et al. [38] studied the effect of temperature on the structure and magnetic properties of $Co_{0.5}Ni_{0.5}Fe_2O_4$ spinel nanoferrites. The synthesised nanoparticle ferrite was produced via a glycol-thermal method. XRD, EDX, SEM, TEM, FTIR, CFM-VSM techniques were usedto the study these ferrites. The results indicate a soft and hard magnetic behaviour of the sample. M. Raza et al. [39] investigated refinement in the structural and magnetic properties of $Co_{0.5}Ni_{0.5}Fe_2O_4$ and its application as laser micro-propellant using ablation confinement.

They studied the structural and magnetic properties of the $Co_{0.5}Ni_{0.5}Fe_2O_4$ samples that were subsequently subjected to thermal treatments for different time durations. The average crystallite sizes of the synthesized samples were found in the range of 24–46 nm. The XRD patterns showed that increase in thermal treatment time resulted in the refinement of the structure whereas the SEM micrographs depicted a uniform particle size distribution of the synthesized material.

S. R. Gibin et al. [40] carried out synthesis and characterization of nickel cobalt ferrite ($Ni_{1-x}Co_xFe_2O_4$) nanoparticles by co-precipitation method with citrate as chelating agent. The main objective of this study deals with the synthesis and characterization of $Ni_{1-x}Co_xFe_2O_4$ (x = 0.3, 0.5, 0.7) by a facile novel co-precipitation method using citrate as chelating agent. The TG/DT analysis was performed for the as-prepared sample which shows the calcination is necessary for the formation of pure nickel cobalt ferrite nanoparticles. From XRD it confirms that $Ni_{1-x}Co_xFe_2O_4$ nanoparticles belong to spinel type. The surface morphology of $Ni_{1-x}Co_xFe_2O_4$ studied through FE-SEM and FE-TEM indicate that the particles are found crystalline and are in cubic shape. The EDAX analysis revealed the presence of Ni, Co, Fe and O. The Zeta potential exposes the good stability of the prepared $Ni_{1-x}Co_xFe_2O_4$ nanoparticles. S. G. Chavan et al. [41] studied micro-wave sintered nickel doped cobalt ferrite nanoparticles prepared by hydrothermal method. They reported a study of the nickel doped cobalt ferrite $Co_{0.9}Ni_{0.1}Fe_2O_4$ that have been synthesized by conventional hydrothermal technique followed by microwave sintering. The $Co_{0.9}Ni_{0.1}Fe_2O_4$ nanoparticles are characterized by X-ray diffraction (XRD), transmission electron microscopy, field emission scanning electron microscopy, particle size analyzer and vibrating sample magnetometer. The XRD spectra show a high degree of crystallinity and also indicate that the diffraction peaks correspond to the cubic spinel structure. The transmission electron microscopy indicating that the crystallite size of $Co_{0.9}Ni_{0.1}Fe_2O_4$ nanoparticles was in the range of 40–75 nm. The nanoparticles show relatively high saturation magnetization of 32.54 emu/g.

Y. Lin et al. [42] studied increased capacitance of porous $Co_{0.5}Ni_{0.5}Fe_2O_4$ for supercapacitor application. They prepared porous $Co_{0.5}Ni_{0.5}Fe_2O_4$ via a simple template-assistant method followed by a post-calcinating treatment. They observed that the porous $Co_{0.5}Ni_{0.5}Fe_2O_4$ sample exhibits excellent electrochemical performances, including the specific capacitance of 113 F g^{-1} at a scan rate of 5 mV s^{-1} in 1 M KOH aqueous electrolytes. They also reported that the sample possesses an excellent cycling stability by 120.05%

growth of its specific capacitance after 1000 cycles. Thus, the porous $Co_{0.5}Ni_{0.5}Fe_2O_4$ sample is a promising pseudocapacitive material for supercapacitors.

J. Feng et al. [43] investigated on effect of chromium substitution on structural and magnetic properties of Nickel-Cobalt ferrite nanoparticles synthesized by co-precipitation method. $Ni_{0.3}Co_{0.7}Cr_xFe_{2-x}O_4$ (x = 0, 0.2, 0.4, and 0.6) nanoparticles were synthesized by co-precipitation method followed by annealing treatment. The structural and magnetic properties of the samples were determined by X-ray diffraction (XRD), Fourier transform infrared (FT-IR) spectroscopy, thermogravimetric and differential scanning calorimetry (TG-DSC) analysis, and a vibrating sample magnetometer (VSM) at room temperature. The XRD patterns revealed a single-phase cubic spinel structure for all the annealed products. Cation distribution by XRD analysis indicated that Cr^{3+} ions preferentially replace Fe^{3+} ions from the octahedral sites due to their favourable crystal field effects; with increasing Cr content, it was observed that Co^{2+} migrated from octahedral sites to tetrahedral sites. The observed decrease in coercivity can be explained by reduction in magneto-crystalline anisotropy that resulted from migration of Co^{2+} ions from B sites to A sites with the increase in Cr content. R. Kesavamoorthi and C. Ramachandra Raja [44] studied structural and magnetic properties of Cobalt and Copper ions mixed Nickel ferrite nanoparticles. Co^{2+} and Cu^{2+} ions mixed nickel ferrite nanoparticles were synthesized by sol-gel auto combustion method. XRD patterns revealed the existence of a single-phase cubic spinel structure. The average grain size estimated from XRD patterns was found to be from 42 to 56 nm. VSM study indicates increase in saturation magnetization and decrease in coercivity. FE-SEM images exhibit particles with spherical shape and size ranges from 37 to 79 nm. The two main metal ion vibrations of ferrites were observed in FT-IR spectra.

G. S. Kumar et al. [45] studied synthesis and characterization of Nickel-substituted Cobalt ferrite nanoparticles using Sol–Gel auto-combustion method and its structural, functional, magnetic and morphological characteristics. It is noted that the average crystallite size decreases from 31 to 27 nm when the nickel concentration increases from 0.02 to 0.06 M, indicative of the incorporation of Ni^{2+} ion in the cobalt ferrite lattice. FTIR analysis shows the presence of M↔O vibration at the tetrahedral and octahedral sites. Micro-Raman spectroscopy shows the stretching vibrations at 486.87 cm^{-1} (E_g) and 696.96 cm^{-1} (A_{1g}), which are the characteristic vibrations of spinel ferrites. Magnetic studies show the variation in saturation magnetization (M_S = 20.25, 9.41, 18.5 emu/g.) and coercivity (H_C = 746.06, 953.03, 885.59 Oe) when the concentration of Ni^{2+} ion increases from 0.02 to 0.06 M. The prepared nanoparticles show a ferromagnetic nature which is attributed to the creation of an antiparallel spin and the magnetic moment created by the cation at tetrahedral and octahedral sites. The surface morphology of samples is imaged by a field emission scanning electron microscope. V. M. Kanevsky et al. [46] investigated on magnetic properties of polycrystalline and amorphous Cobalt- and Nickel-ferrite films. The magnetic properties of polycrystalline and amorphous cobalt- and nickel-ferrite films obtained by solid-phase synthesis were studied. Polycrystalline nickel-ferrite films are shown to be characterized by significant coercive fields at room temperature in the direction normal to the substrate plane. Compressive stresses that arise in the films during solid-phase oxidation and synthesis are assumed to contribute to the enhancement of the coercive fields. X-ray amorphous films have only paramagnetic properties.

B. Nandan et al. [47] investigated cation distribution in nanocrystalline cobalt substituted nickel ferrites. Nanocrystalline $Ni_{1-x}Co_xFe_2O_4$ (x = 0.0, 0.4, 0.5, 0.6, 1.0) samples were synthesized using sol-gel technique. X-ray diffraction (XRD) and vibrational spectroscopy techniques were employed to study the structure, cation distribution and ordering in the Co^{2+} substituted nickel ferrite (NCFO) samples. The XRD analysis of the specimen confirmed the formation of single cubic spinel phase. Infrared and Raman spectroscopies too confirmed the spinel phase formation in the samples. It is revealed that nickel ferrite (NFO) is nearly inverse (96% Ni^{2+}on B-sites). The substitution of Co^{2+} in NFO results into a partially inverse mixed ferrite phase with Co occupying nearly 18% A-sites in $Ni_{0.5}Co_{0.5}Fe_2O_4$and 25% in $CoFe_2O_4$.

Mayara dos Santos Amarante et al. [48] studied sintering behaviour and electromagnetic properties of a Ni-Co ferrite/NiO biphasic ceramic. In this work, a biphasic ferrite-based ceramic was produced by the standard ceramic method, starting from iron, nickel, and cobalt oxides as raw materials with a (Ni+Co):Fe atomic proportion of 1.3:1.7. The EDS microanalysis and X-ray diffractometry of the sintered sample revealed the presence of a major fraction of ferrite phase (estimated as $Ni_{0.8}Co_{0.2}Fe_2O_4$) and a NiO. CoO second phase with NiO in majority. The results suggest that adjustment of the oxides' proportion on the formulation step of the ferrite processing is a simple an effective way of tailoring the electromagnetic properties of the ferrite.

1.6 Aim, Objective and Plan of work.

The aims and objective of the study is to select a definite ferrite composition, $Co_{0.5}Ni_{0.5}Fe_2O_4$ and synthesis it to obtain 'as prepared' ferrite which is to be subjected at different sintering temperature and study the effect on various structural, electric, dielectric and magnetic properties of sintered ferrites. The synthesised was planned by combustion method using D-malic acid as fuel and optimizing the condition for combustion reaction between metal nitrates and fuel which is to be examined by XRD.

It is planned to study 'as prepared' ferrite and 'sintered' ferrites by characterising them using various technique such as x-ray diffractometry, IR, scanning electron microscopy, transmission electron spectroscopy and studying their structural, electric, dielectric and diamagnetic properties.

In summary the main aim of this research work has been to study the influence of different sintering temperature on structural and solid state properties of $Co_{0.5}Ni_{0.5}Fe_2O_{4.}$

CHAPTER-II

EXPERIMENTAL TECHNIQUES AND CHARACTERISATION

2.1 EXPERIMENTAL TECHNIQUE:

PREPARATION OF FERRITES BY COMBUSTION METHOD

2.1.1 Optimisation of synthesis method

In order to get nanosized particles of $Co_{0.5}Ni_{0.5}Fe_2O_4$, different ratios of oxidizer to fuel were used so as to know most optimum ratio apart from the formation of stoichiometric ferrites.

The cobalt nickel ferrite having composition $Co_{0.5}Ni_{0.5}Fe_2O_4$ was prepared by combustion method using D-malic acid ($C_4H_6O_5$) as fuel. By taking various ratios of oxidizer:fuel, ferrites were prepared. The oxidiser used are metal nitrates namely cobalt nitrate, nickel nitrate and ferric nitrate. The amount of metal nitrates was kept constant and amount of fuel was varied. The oxides formed were than analysed by XRD and from the XRD data the best ratio was selected. The best ratio selected was based on the oxides that showed single phase, broad peaks, less intensity without any impurity peaks. By using the selected ratio the main series of the ferrites was prepared. The amount of different metal nitrates and fuel taken is listed in the Table 1**.**

Table 1: The amounts of different metal nitrates and fuel taken along with oxidiser:fuel ratio taken for optimization

Sr No	$Co(NO_3)_2.6H_2O$ g	$Ni(NO_3)_2.6H_2O$ G	$Fe(NO_3)_3.9H_2O$ g	($C_4H_6O_5$) g	Oxidiser:Fuel
1	1.7820	1.7624	9.7939	2.0524	1:0.417
2	1.7820	1.7624	9.7939	2.7365	1:0.556
3	1.7820	1.7624	9.7939	3.4207	1:0.694
4	1.7820	1.7624	9.7939	4.1048	1:0.833
5	1.7820	1.7624	9.7939	4.7890	1:0.972
6	1.7820	1.7624	9.7939	5.4731	1:1.111
7	1.7820	1.7624	9.7939	6.1571	1:1.25
8	1.7820	1.7624	9.7939	6.8413	1:1.389
9	1.7820	1.7624	9.7939	7.5255	1:1.528
10	1.7820	1.7624	9.7939	8.2096	1:1.667

The X-ray diffraction patterns were recorded of all the ferrite samples and the same have been shown in Fig.1. It is observed that the oxidizer: fuel ratio of 1:1.111 forms a single phase, cubic spinel structure with broad peaks which is an indication of nano size particles formation. Thus ratio 1:1.111 was selected for the synthesis of the rest of the ferrite samples.

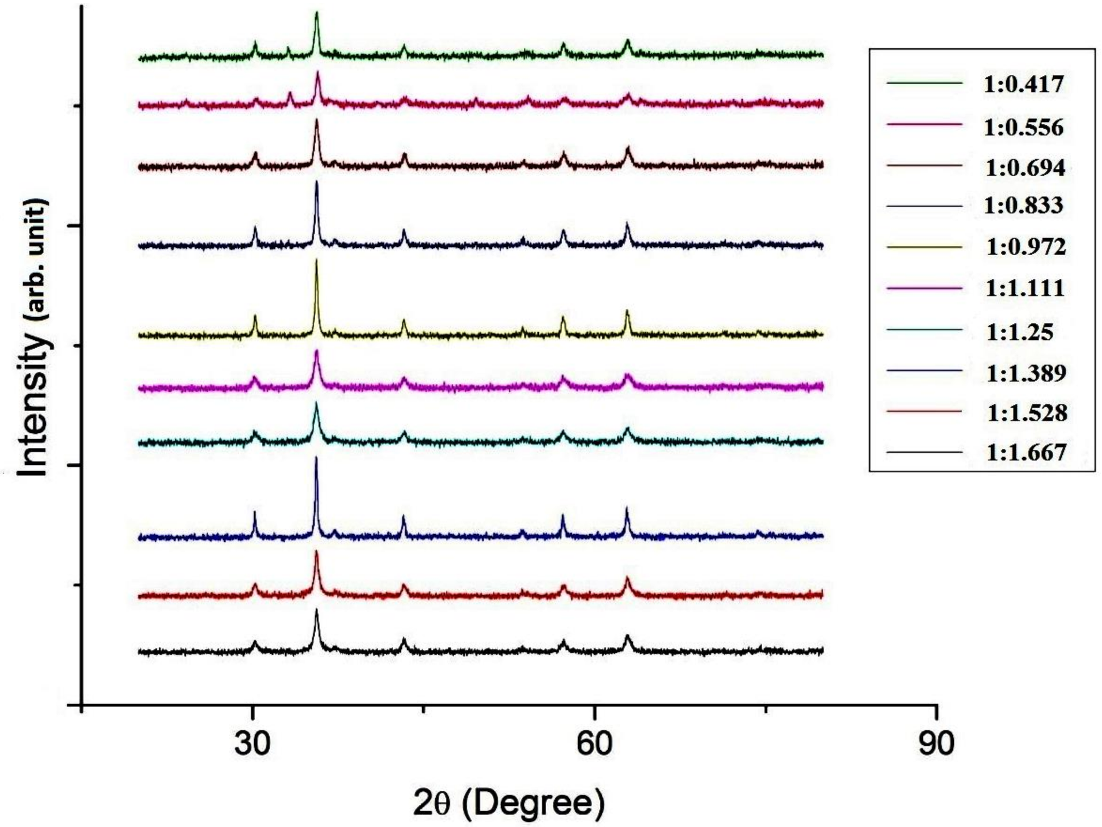

Figure 1. XRD powder pattern of $Co_{0.5}Ni_{0.5}Fe_2O_4$ prepared by varying O:F ratio.

2.1.2 Synthesis of $Co_{0.5}Ni_{0.5}Fe_2O_4$ by combustion method

Stoichiometric amount cobalt Nitrate [$Co(NO_3)_2.6H_2O$] , nickel Nitrate [$Ni(NO_3)_2.6H_2O$] and ferric nitrate [$Fe(NO_3)_3.9H_2O$] were taken and kept on the hotplate to form the melt. This melt was allowed to cool and then to it was added D-malic acid. The fuel was added in such an amount that the oxidizer to fuel ratio was maintained as 1:1.111. The whole mixture was slowly heated with stirring in between until it formed homogenous sticky slurry. Further heating attains ignition temperature of the mixture, where it catches fire and slow combustion to form a desired Nanocrystalline single phase ferrite powder. Finally the powder was calcinated at 500^0C for 5 hours to remove any unburned species remained, if any. The amount of the metal nitrates and the fuel taken for the synthesis is given in Table 2.

Table 2: Amount of metal nitrates and D-malic acid taken for the preparation of $Co_{0.5}Ni_{0.5}Fe_2O_4$

Composition	$Co(NO_3)_2.6H_2O$ (g)	$Ni(NO_3)_2.6H_2O$ (g)	$Fe(NO_3)_3.9H_2O$ (g)	$C_4H_6O_5$ (g)	O:F
$Co_{0.5}Ni_{0.5}Fe_2O_4$	1.7820	1.7624	9.7939	5.4731	1:1.111

Chemical Equation:

$$0.5Co(NO_3)_2.6H_2O + 0.5Ni(NO_3)_2.6H_2O + 2Fe(NO_3)_3.9H_2O + C_4H_6O_5$$

$$\downarrow$$

$$Co_{0.5}Ni_{0.5}Fe_2O_4 + x\ CO_{2\ (g)}\uparrow + x\ NO_{X\ (g)}\uparrow + xH_2O_{(g)}\uparrow$$

The ferrites obtained were ground for 2 hours to get the fine powder. This fine powder obtained is called as the **"AS PREPARED" FERRITE.**

Preparation of pellets: 0.7g of 'as prepared' ferrite was weighed and pressed in the circular shaped conventional die using hydraulic press by applying 3 tonnes of pressure for 3 minutes.

2.1.3 Sintering of ferrites

Sintering is done to control the extrinsic properties of the ferrites which involves two stages namely pre-sintering and final sintering.

Presintering

The "AS PREPARED" powder pellets were taken in silica crucibles and were heated to 700 °C for 5 hours in muffle furnace.

The main purpose of Pre-sintering:

- To reduce the shrinkage which takes place during final sintering
- Helps in homogenizing the material
- To decompose any carbon or higher oxides, if present. This reduces the evolution of gas in final sintering.

Final Sintering

Pre-sintered pellets were thoroughly grinded for 2 hours. The fine particles were made in order to reduce the particle size and to promote mixing of remaining unreacted oxides. After grinding for 2 hours, pellets were prepared by applying pressure of 3 tonnes/inch^2 for 3 minutes in hydraulic press. The pellets prepared were then sintered at 6 different temperatures 800 °C 850 °C, 900 °C, 950 °C, 1000 °C and 1050°C for 10 hours in furnace. The final sintering increases the density and the particle size while decreasing the porosity of the material. These pellets and powder of "AS PREPARED" and "SINTERED" ferrites were then used for further characterisation and to study their solid state properties.

2.2 Characterisation Technique

The “AS PREPARED” and “SINTERED” ferrites at six different temperatures were studied using different technique and their solid state properties were studied. The characterisation is important to know the chemical identity of the materials. The different characterisation techniques used in the present studies were XRD, SEM and FTIR. The detail of characterisation techniques are given below.
A comparison between nanosized particle and bulk of these materials was done.

2.2.1 Chemical Analysis

Chemical analysis is the study of the chemical composition which involves the determination of the percentage of metal ions present in the ferrite sample.

a. Preparation of stock solution

0.5 g of ‘AS PREPARED’ $Co_{0.5}Ni_{0.5}Fe_2O_4$ was weighed and to it 10 mL of 9M HCl was added followed by few drops of H_2O_2 in a beaker on hot plate. Reaction mixture was heated by same procedure till the oxide decomposes completely and was then extracted by using 9M HCl.

b. Separation using anion exchange resin

The IR Amberlite 400 resin was soaked overnight in 9M HCl and was used for the separation of ions. The column was washed with 150 mL of 9M HCl and the flow rate was adjusted to 4-5 mL per minute. 10 mL of the stock solution was added to the column containing 9M HCl.

The Nickel ions were eluted from the column using 80 mL of 9M HCl and effluents were collected in 250 mL volumetric flask which was diluted up to the mark using acidified water and was used for Ni^{+2} estimation.
The cobalt ions were eluted by using 75 mL of 4M HCl and was collected in 250 mL volumetric flask which was diluted up to the mark using acidified water and was used for Co^{+2} estimation.
The ferric ions were eluted by using 100 mL of 0.5M HCl and was collected in 250mL volumetric flask which was diluted up to the mark using acidified water and was used for Fe^{+2} estimation

c. Determination of Cobalt

25 mL of Cobalt stock solution was taken and to it 10mL of distilled water was added followed by addition of Hexamine till pH = 6. To it was then added 3-4 drops of Xylenol orange indicator. This reaction mixture was titrated against 0.01M EDTA. The colour change observed was wine red to yellow.

d. Determination of Iron

To the iron stock solution, 7g of NH_4Cl was added which was allowed to dissolve followed by dropwise addition of 2N NH_4OH till the pH= 6. The reddish brown precipitate of $Fe(OH)_3$ formed was digested for 20min on water bath. The precipitate obtained was filtered and then was transferred to pre weighed silica crucible for decomposition at 600 ^{0}C for 15-20 minutes. The colour of the precipitate changed to red indicating the formation of Fe_2O_3.

e. Determination of Nickel

25 mL of nickel solution was taken and to it 100mL of distilled water was added followed by addition of solid murexide indicator and l0mL of the 1M ammonium chloride solution along with concentrated ammonia solution dropwise until the pH=7 (yellow colour of the solution). This reaction mixture was titrated against 0.01 M EDTA until the end point was approached, then render the solution strongly alkaline by the addition of 10mL of concentrated ammonia solution, and the titration was continued until the colour changed from yellow to violet.

2.2.2 X-ray diffraction studies

The crystal structure and phase purity of all the composition was determined by X-Ray Diffraction technique using Philips-PW 3710 diffractometer with Cu-Kα radiation and Ni filter.

The X-ray diffraction technique was used:

1. To confirm the formation of single phase.
2. To confirm whether the solid state reaction is completed or not
3. To find the lattice parameter, porosity and crystallite size.

- **Bragg's law** : When a monochromatic X-rays are incident upon a crystal, atoms in different layers acts as a source of scattering radiation of same wavelength. The intensity of the reflected beam will be maximum at certain incident angle when the path difference between two reflected wave from two different planes is an integral multiple of wavelength of X-rays.

The identification of crystalline phase in a powder pattern depends on two types of information.

1. The interplanar distances of diffraction planes (h, k, l) known as 'd' spacing.
2. The relative intensity for each 'd' spacing.

According to Bragg's law, the diffraction maximum is obtained if

$$n\,\lambda = 2d\sin\theta_{hkl}$$

θ= Glancing angle

n= Order of reflection

d= Interplanar spacing

λ= Wavelength of X-ray1

- The lattice constant 'a' for the cubic crystal system was calculated using equation

$$a = d\sqrt{h^2 + k^2 + l^2}$$

Where h, k, l are the miller indices of the diffraction peaks and 'd' is the interplanar distance.

- The crystallite size was determined using Scherrer formula

$$\boldsymbol{t = \frac{0.9\,\lambda}{\beta cos\theta}}$$

t= Thickness of crystal

λ= X-ray wavelength

$\theta =$ Bragg's angle

β= full width at half maximum in radians

- The porosity (P) of the ferrite sample was determined using formula

$$\mathbf{P = 1 - \frac{dm}{dx}}$$

- The measured density (dm) was calculated using

$$\mathbf{dm = 1 - \frac{m}{\pi r^2 h}}$$

h= Height of the pellet
r= Radius of the pellet
m= Mass of the pellet

- The theoretical density (dx) was calculated by using formula

$$\mathbf{dx = \frac{8M}{NV}}$$

8= Number of formula unit cell
N= Avogadro’s number
V= Volume of the unit cell which is equal to a^3
For spinel cubic system
M= Mass of the pellet

2.2.3 Infrared studies

For a molecule to absorb in IR region, the vibration or rotation within a molecule must cause a net change in dipole moment. The IR spectra of all the samples were recorded on Shimadzu FTIR-IR prestigue-21 spectrophotometer. A small amount of sample was mixed with KBr and the spectra were recorded in frequency range 350 cm^{-1} to 4000 cm^{-1} at room temperature.

2.2.4 Scanning Electron Microscopy

The surface morphology of the “AS PREPARED” and “SINTERED” ferrite samples was recorded on ZEISS model 5800L scanning electron microscope. The aim of the SEM studies was to find out the growth and homogeneity of the samples and also to find out the variation in the particle size as the sintering temperature increases.

2.3 Study of the solid state properties

2.3.1 Electrical studies

A. DC Electrical Resistivity

The electrical resistivity of ferrite samples were carried out using the two probe DC method in the temperature range of around room temperature to 500 ^{0}C. The pellets of diameter 10 mm and 3 mm thickness were pressed between the two electrodes and the measurements were carried out. The voltage was kept constant and the current was measured and using the Ohm’s law the resistance was calculated.

The resistance obtained was used to find out the resistivity of the sample by using the relation

$$\boldsymbol{\rho = \frac{Ra}{t}}$$

R=Resistance

a = Cross sectional area of the pellet

t = Thickness of the pellet

B. Seebeck Coefficient/ Thermoelectric Power

The thermoelectric properties are widely used in the interpretation of the conduction mechanism in semiconductors to know whether it is p-type or n-type. Seebeck coefficient measurements were carried out by using four probe setup by developing pressure difference of 20 K-30 K across pellet and corresponding voltage was measured from room temperature to 500 ^{0}C.

The seebeck coefficient α is given by equation

$$\boldsymbol{\alpha = \frac{\Delta V}{\Delta T}}$$

ΔV =Voltage developed across the sample

ΔT = Temperature difference across the sample

2.3.2 Dielectric studies

The dielectric measurement were carried out by two probe method using a Wayne Kerr 6500P LCR meter in the frequency range of 20 Hz to 10 MHz. The dielectric material increases the storage capacity of the capacitors by neutralising charges at the electrodes which ordinarily would contribute to the external field. The samples were pressed into circular disc shaped pellets, and silver coating was done on adjacent faces for better conduction.

- The dielectric constant of the ferrites sample was calculated by using the relation,

$$\boldsymbol{\varepsilon' = \frac{Ct}{\varepsilon_0 A}}$$

ε’= Dielectric constant

ε_o= Free space permittivity (8.854 *10^{-12} F/m)

C= Capacitance of the sample in F

t= Thickness of the specimen

- The dielectric loss tangent (tan d) was calculated by using the relation

$$\tan \delta = D \qquad \text{D= Dissipation factor}$$

2.4 Magnetic Studies

2.4.1 AC susceptibility study

The AC susceptibility studies are carried out to find out the Curie temperature and domain structure of the ferrite samples. It also reveals the ferromagnetic to paramagnetic transitions. The data of normalized susceptibility against the temperature was plotted for all the samples. The AC susceptibility measurements were carried out on powdered samples by using the Set-up supplied by ADEC Embedded Technology & Solutions Pvt Ltd, Corlim-Goa, India. The data of normalised AC susceptibility against temperature was plotted for all the ferrites.

CHAPTER-III

RESULT
AND
DISCUSSIONS

3.1 Characterisation and solid state properties of $Co_{0.5}Ni_{0.5}Fe_2O_4$ sintered at different temperature

The $Co_{0.5}Ni_{0.5}Fe_2O_4$ was prepared by combustion method as described in section 2.1 of Chapter 2. These ferrites were assigned sample code as given in Table 3.

Table 3: Sample codes for the "AS PREPARED" and "SINTERED" $Co_{0.5}Ni_{0.5}Fe_2O_4$

Composition	Sintering Temperature (^{0}C)	Sample Code
$Co_{0.5}Ni_{0.5}Fe_2O_4$	AS PREPARED	CNF AP
	800	CNF 800
	850	CNF 850
	900	CNF 900
	950	CNF 950
	1000	CNF 1000
	1050	CNF 1050

3.1.1 Chemical Analysis

The chemical analysis of the "AS PREPARED" ferrite sample was carried out in order to confirm the stoichiometry of the ferrite synthesized. The theoretical and the experimental amount of the metal ion present in CNF AP is given in Table 4 and from this Table it can be concluded that the experimental percentages for all the three metal ions i.e. Cobalt, Nickel and Iron matches very well with the theoretical data confirming the predicted formula for CNF AP.

Table 4: The Theoretical and Experimental percentages of cobalt, nickel and iron present in CNF AP

Sample code	% of Cobalt		% of Nickel		% of Iron	
	Experimental	Theoretical	Experimental	Theoretical	Experimental	Theoretical
CNF AP	12.01	12.56	11.99	12.51	45.37	47.63

3.1.2 XRD analysis

Figure 2 shows the XRD patterns of the as-synthesized $Co_{0.5}Ni_{0.5}Fe_2O_4$ ferrite sample prepared by the combustion method and calcined at 500 ^{0}C.

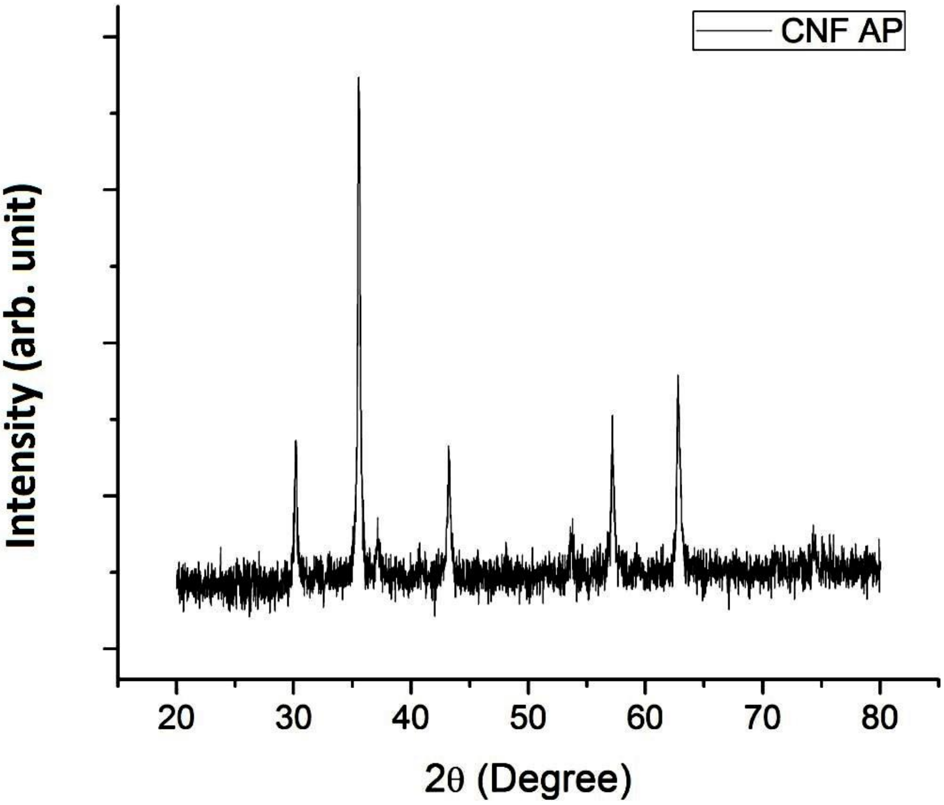

Fig. 2. XRD pattern of 'as prepared' $Co_{0.5}Ni_{0.5}Fe_2O_4$ ferrite sample

The formation of monophasic $Co_{0.5}Ni_{0.5}Fe_2O_4$ nanoparticles was confirmed from the XRD pattern shown in Figure 2. The XRD pattern demonstrates the formation of single cubic spinel phase. In other words, no secondary phase was detected in XRD pattern which ensures the phase purity of the sample. The dominant peak is centred at $2\Theta = 35.54^o$ which corresponds to crystal plane (311). This peak is characteristic peak of face centred cubic spinel. The different parameters such as Lattice Parameter 'a', measured density 'dm', theoretical density 'dx', porosity 'P', and crystallite size 't' was calculated using this XRD pattern for CNF AP and the same are given in Table 5.

Table 5. Lattice parameter 'a', measured density 'dm', theoretical density 'dx', porosity 'P', and crystallite size 't' of the CNF AP.

Sample Code	Lattice parameter (Å)	Measured Density 'dm' (g/cm^3)	Theoretical Density 'dx' (g/cm^3)	Porosity 'P'	Crystallite Size 't' (nm)
CNF AP	8.359	2.9723	5.3330	0.4426	28

3.1.3 IR studies

The IR spectra of the CNF AP was recorded in the range of 350–4000 cm^{-1} and the same has been shown in Figure 3. From this figure we can see that it shows two distinct M-O stretching vibrations of spinel ferrite in the range 350–700 cm^{-1} [49, 50].

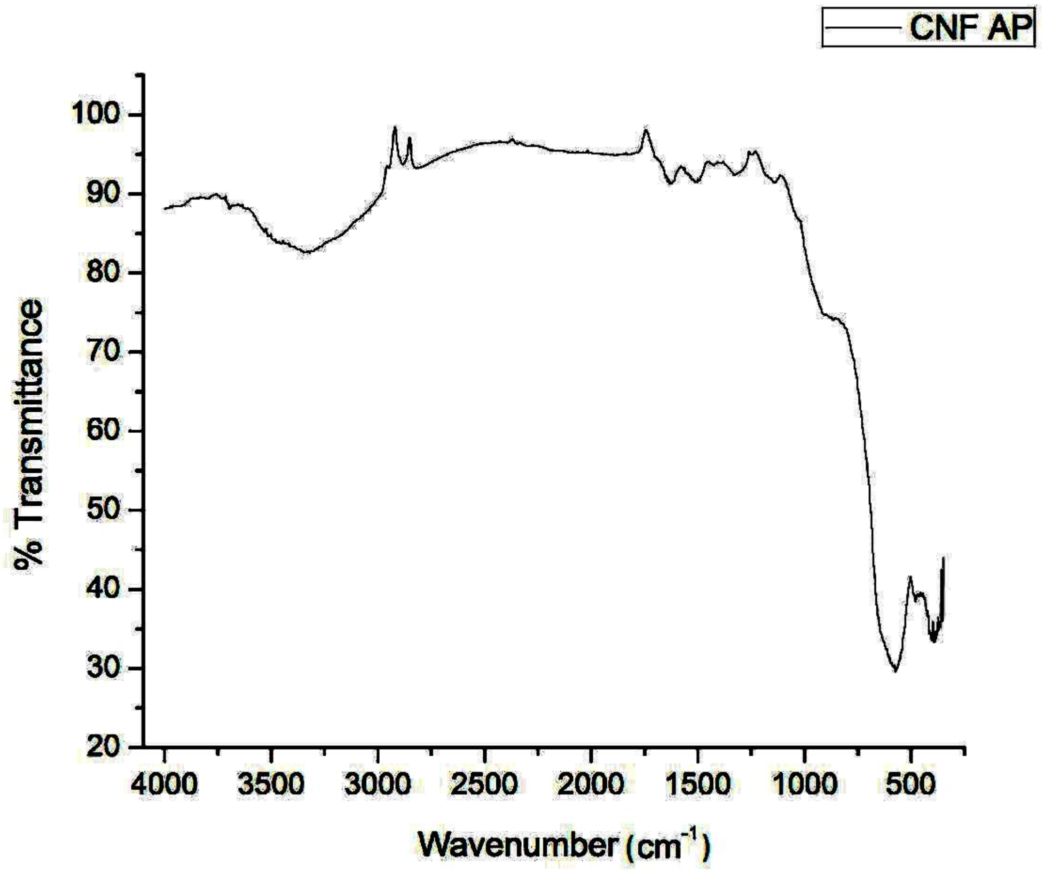

Fig. 3. IR spectra of 'as prepared' $Co_{0.5}Ni_{0.5}Fe_2O_4$ (CNF AP) ferrite sample.

The higher band stretching vibrations at 592 cm^{-1} is due to intrinsic stretching vibrations of metal-oxygen (Fe↔O) at tetrahedral site (ν_1) while the lower bands at around 363 cm^{-1} is due to M-O stretching vibrations (Ni↔ ↔O and Co ↔O) at octahedral sites (ν_2) as observed in earlier reported literature [31, 35, 50]. An infrared spectroscopy study indicate the presence of tetrahedral and octahedral group complexes, respectively, within the spinel phase [31, 41, 50]. The positional difference between tetrahedral and octahedral vibrations is because of the

Fe^{3+} -O^{2-} bond distance between octahedral and tetrahedral sites [52]. The band at ~3400 cm^{-1} corresponds to –OH group due to adsorbed water [38].

3.1.4 SEM studies

The SEM micrographs of “AS PREPARED” and the “SINTERED” $Co_{0.5}Ni_{0.5}Fe_2O_4$ ferrite samples are shown in Figure 4 a and b, respectively.

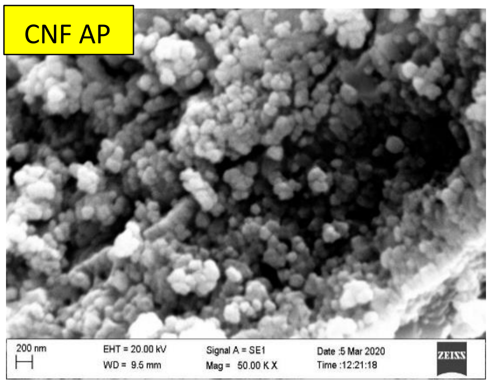

Fig. 4a. SEM micrograph of ‘AS PREPARED’ $Co_{0.5}Ni_{0.5}Fe_2O_4$ ferrite sample

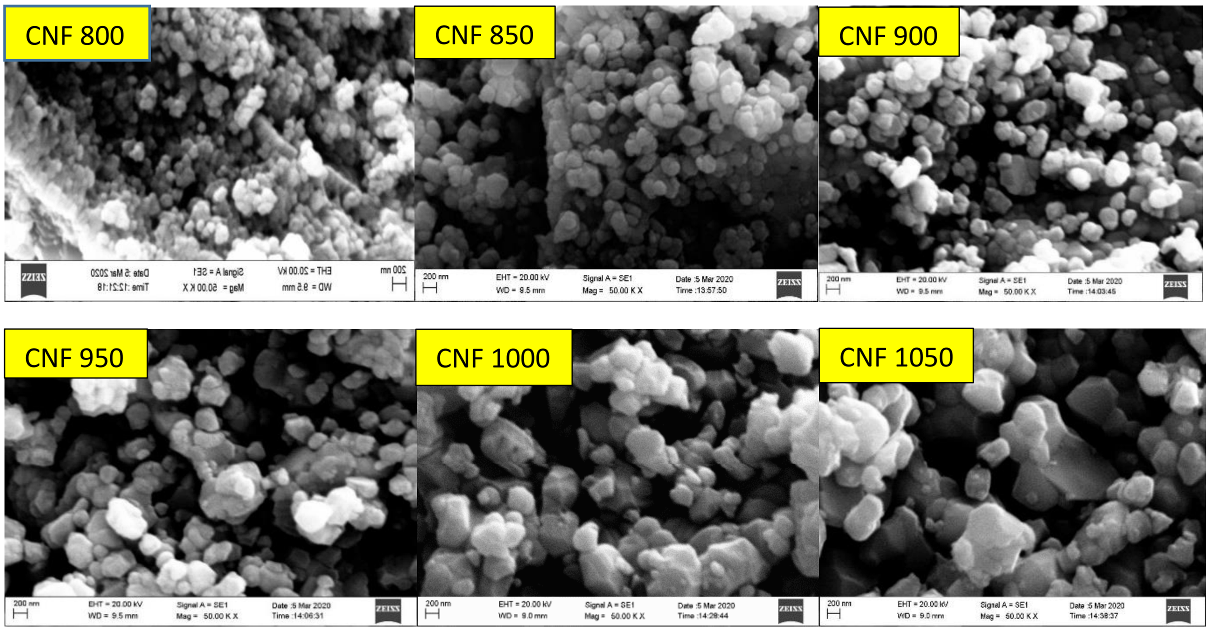

Fig. 4b. SEM micrographs of ‘sintered’ $Co_{0.5}Ni_{0.5}Fe_2O_4$ ferrite samples.

The SEM images given in Figure 4a and 4b shows the spherical type of morphology with a high degree of agglomeration of particles resulting in uneven size distribution over a wide range. The micrographs of “Sintered” Ferrite as shown in Fig 4b revealed that the ferrite samples are composed of nanoparticles with a high degree of agglomeration. The high degree of agglomeration can be attributed to the magnetic nature of the samples [54]. These images shows a clear evidence that the extent of agglomeration increases with increase in sintering temperature which results in aggregation of small crystallites forming bigger particles. The similar trend was observed in the earlier reported literature [50].

3.2 Study of solid state properties of $Co_{0.5}Ni_{0.5}Fe_2O_4$ at different sintering temperature

3.2.1 Electrical studies

A. DC Electrical Resistivity

DC electrical resistivity of the “as prepared” ferrite was carried out using 2-probe technique in the temperature range of 333–768 K with the use of 10 mm pellet as a sample. The graph of Log ρ vs 1000/T (K^{-1}) was plotted and is given in Figure 5. It was observed that with an increase in temperature, the resistivity goes on decreasing showing a semiconducting behaviour. This is because, although the net charge carriers’ concentration stays almost similar over the temperature range in ferrites, the hopping frequency associated with charge carriers rises with temperature. Also, there is an increase in the drift mobility of thermally activated charge carriers at elevated temperatures which is dependent on grain size, density, porosity, and composition and contributes to a decrease in resistivity [52].

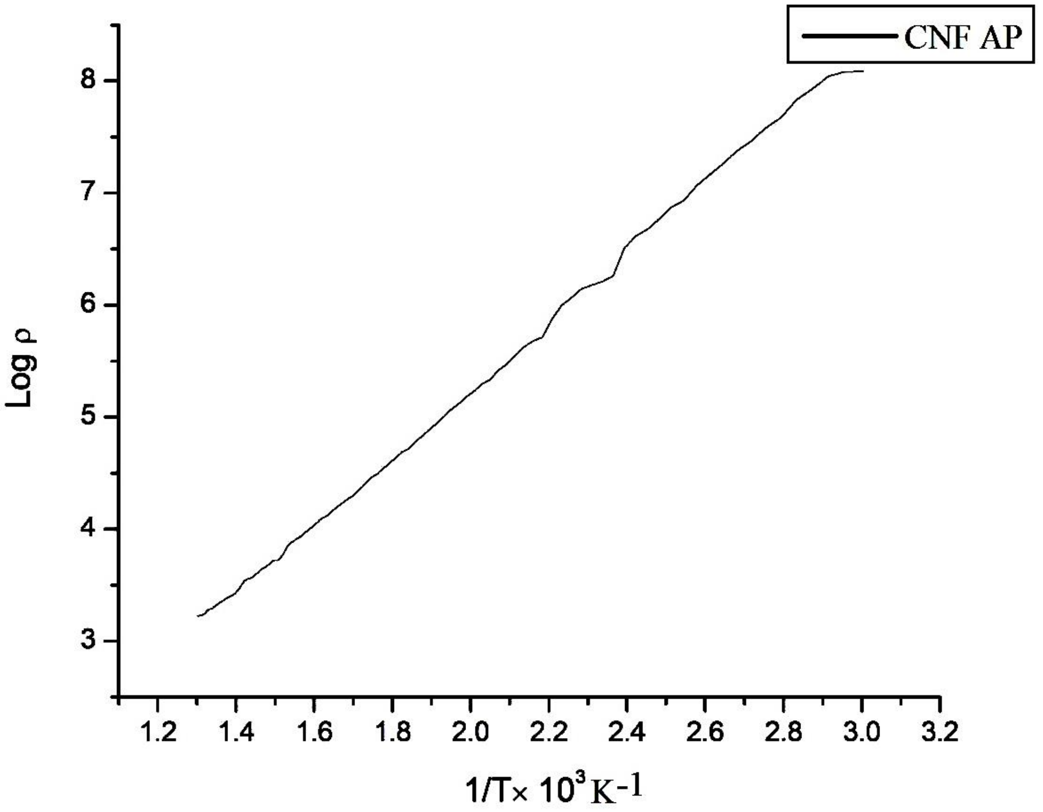

Figure 5: The plot of Log ρ versus 1/T*1000 of CNF AP

B. Thermoelectric Power studies

The plots of Seebeck coefficient against temperature of ‘as prepared’ and ‘sintered’ $Co_{0.5}Ni_{0.5}Fe_2O_4$ ferrite sample investigated from room temperature till 500 ^{0}C is given in Fig 6a, 6b and 6c.

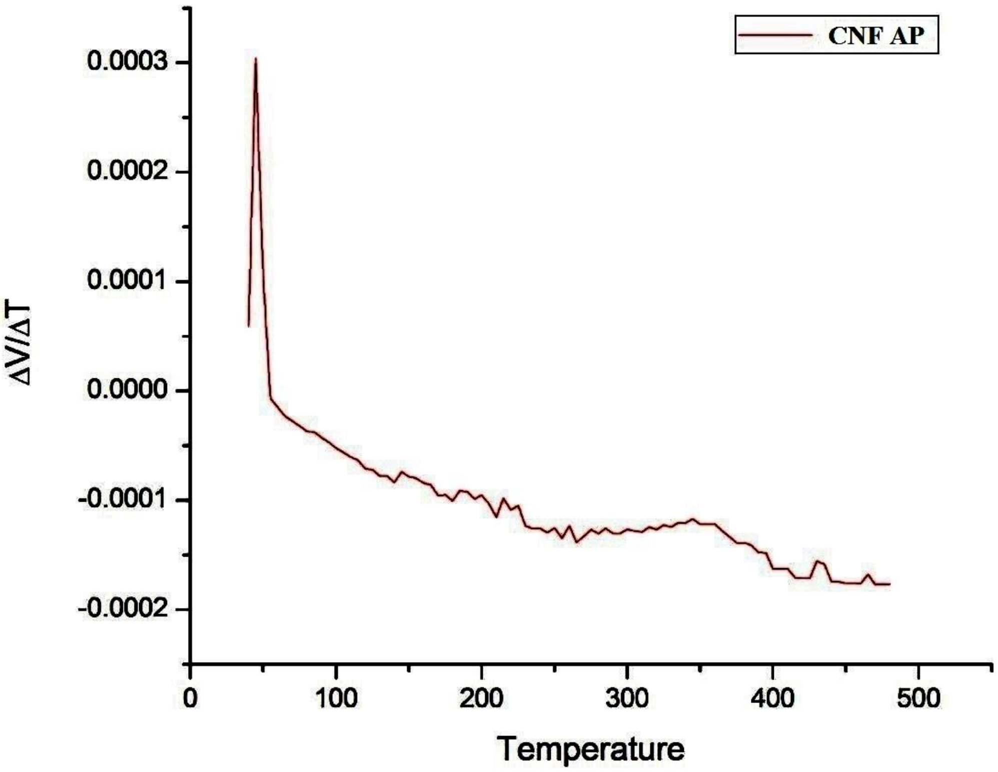

Fig. 6a. The plot of Seebeck coefficient versus temperature of CNF AP

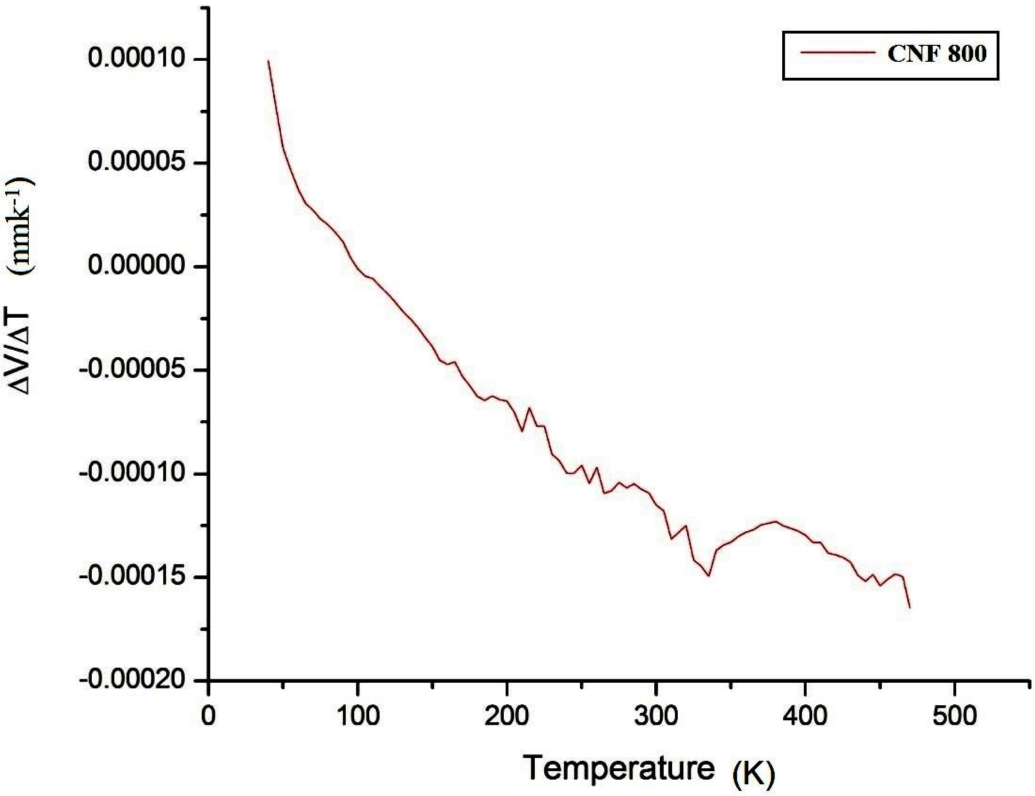

Fig. 6b: The plot of Seebeck coefficient versus temperature for CNF 800

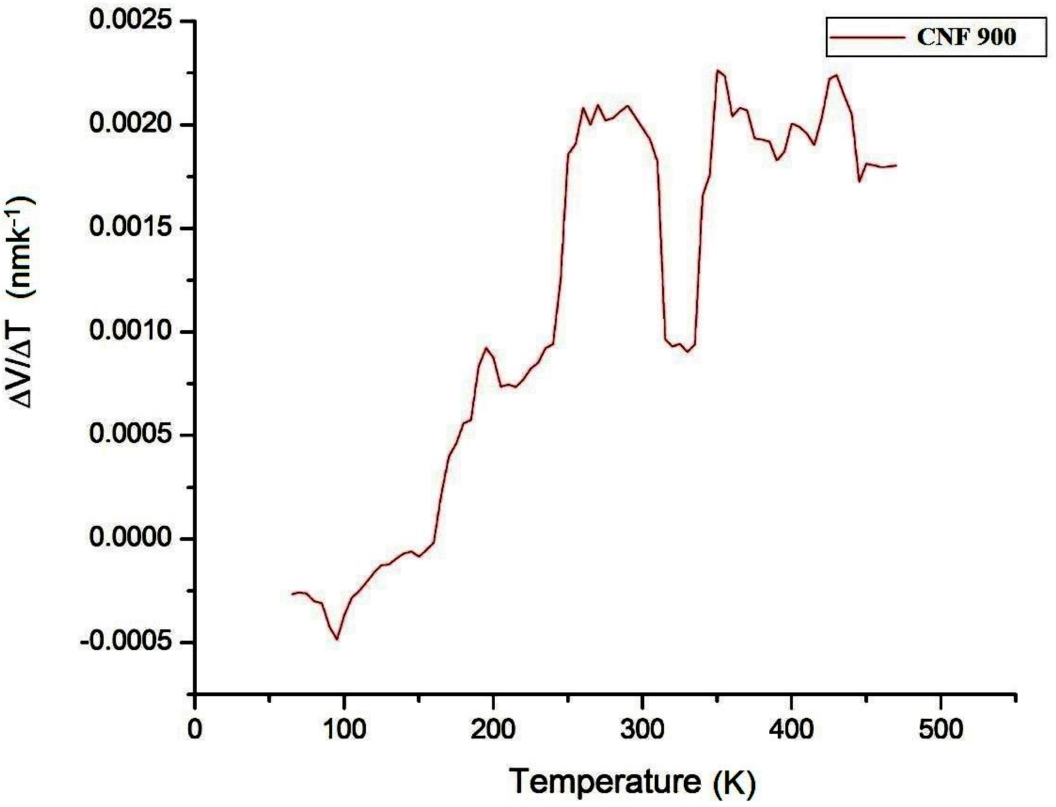

Fig. 6c. The plot of Seebeck coefficient versus temperature for CNF 900

It is observed from Figure 6a and b that CNF AP and CNF 800 shows positive Seeback coefficient initially at room temperature which then changes to negative thermoemf value at higher temperature indicating n-type semiconductor which means that the charge carriers are electrons whereas CNF 900 initially shows n-type semi conduction which is then changed to p-type semi conduction at higher temperature indicating that the charge carriers are holes as shown in Figure 6c. These type of trends are reported by other researchers also [53].

3.3.2 Dielectric studies

The Fig. 7 shows variation of dielectric constant as a function of frequency of the “AS PREPARED” and “SINTERED” ferrite samples of the $Co_{0.5}Ni_{0.5}Fe_2O_4$ at room temperature from 20 Hz to 10 MHz. It is observed from Fig. 7 that with increase in frequency, the dielectric constant decreases for all the compositions. The decrease in dielectric constant with increasing frequency is a normal behaviour observed in spinel ferrites which is due to interfacial polarisation as predicted by Maxwell–Wagner [30]. This decrease is more at lower frequencies than at higher frequencies. Such behaviour of ε' can be understood by exploring the layered structure of ferrites. Ferrites are basically composed of well conducting grains separated by thin layer of poorly conducting grain boundaries. These grain boundaries are formed during sintering process due to direct contact of material with the firing atmosphere, crystallites get oxidized, leading to the formation of grain boundaries. At lower frequencies, the grain boundaries dominate the grains in deciding the dielectric properties. With increase in frequency, role of grain boundaries starts decreasing while that of grains starts increasing, which has resulted in more variation in ε’ with frequency .Conductivity difference between grains and grain boundaries leads to the accumulation of charge carriers at boundaries, which leads to generation of space charge polarization. As a result, net polarization increases and hence higher values of ε' are obtained at lower frequencies. Similar type of trend was noted in earlier report [54].

The dielectric properties are also affected by grain size. Ferrite with small grains contains large number of surface boundaries, which means high resistance is faced by the charge carriers. This leads to reduction in interfacial polarization and hence in dielectric constant [54]. This is the reason why lower values of dielectric constant are observed.

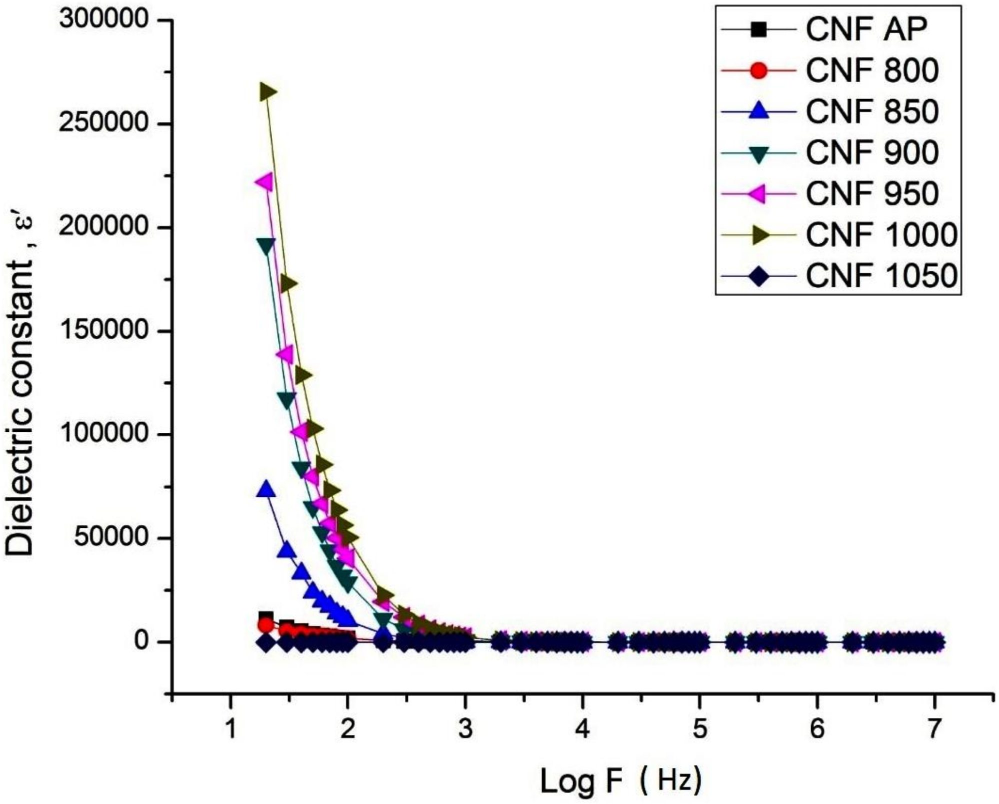

Fig. 7. The plot of dielectric constant v/s Log F of the “AS PREPARED” and “SINTERED” $Co_{0.5}Ni_{0.5}Fe_2O_4$ ferrite.

The variation of dielectric loss as a function of frequency for the “AS PREPARED” AND “SINTERED” $Co_{0.5}Ni_{0.5}Fe_2O_4$ ferrite at room temperature from 20Hz to 10MHz is shown in Fig. 8.

The dielectric loss gives the loss of energy from the applied field into the sample. This is caused by domain wall resonance. At higher frequencies, the losses are found to be low, since domain wall motion is inhibited and magnetization is forced to change rotation. The dielectric dispersion curve can be explained on the basis of Koop’s theory [51], based on the Maxwell–Wagner model for the inhomogeneous double structure.

The dielectric losses basically represent the energy dissipation in the dielectric medium and depend on the number of ferric and ferrous ions in the material. It can be seen that dielectric loss decreases with frequency. At lower frequencies, grain boundaries are dominating. Therefore, more energy is required for electron exchange between ferric and ferrous ions $Fe^{+2} \leftrightarrow Fe^{+3}$ which leads to high energy losses. With increase in frequency, role of grain boundaries starts decreasing, hence energy losses start decreasing [54]. The maximum dielectric losses are obtained for composition CNF 950 in the scanned frequency range.

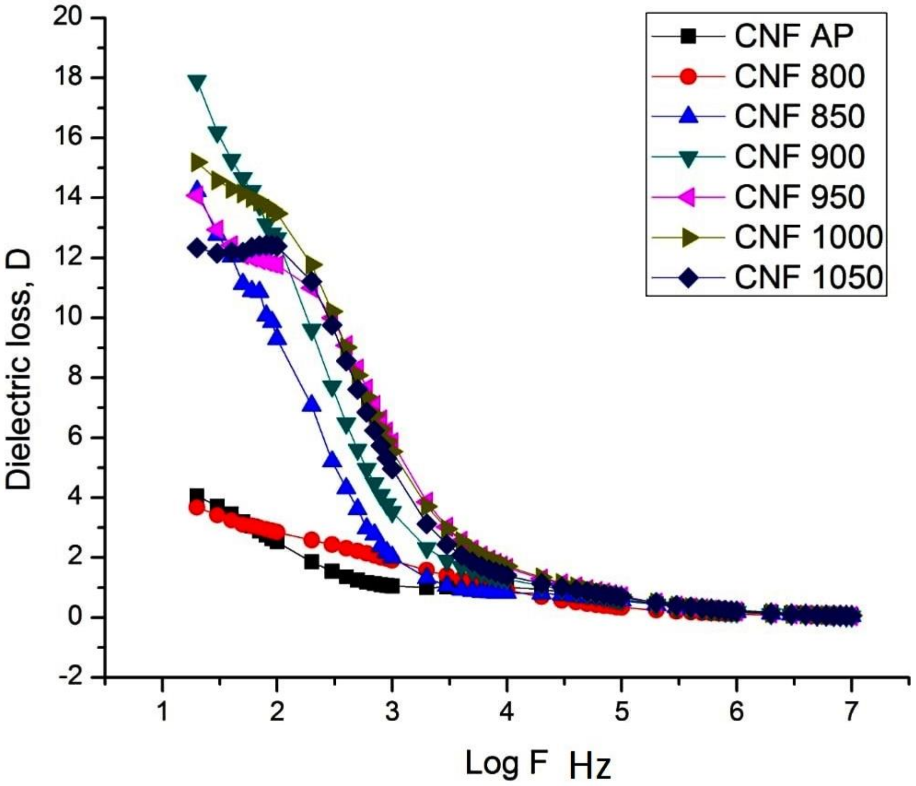

Fig. 8. The plot of Dielectric loss versus Log F of “AS PREPARED” and “SINTERED” $Co_{0.5}Ni_{0.5}Fe_2O_4$ ferrite

3.3 Magnetic properties

3.3.1 AC Susceptibility studies

The alternating current susceptibility studies of the 'as prepared' and "sintered" nanoparticle ferrites were measured in the temperature range of 25^0C until the Curie point is attained. This study allows us to discuss on the different available domains state in the materials on the basis of particle size distribution. T_c is the characteristic magnetic transition temperature which gives an idea about the amount of energy required to disturb the magnetic ordering in the magnetic material. The shape of curves observed with the change in temperature gives the information about the domain states i.e. super paramagnetic (SP), single domain (SD) or multi domain (MD).

The Curie temperature from the AC susceptibility study is determined by extrapolating the steady decrease in susceptibility to intercept with the X-axis, and also from the subsequent fall in susceptibility to zero values.

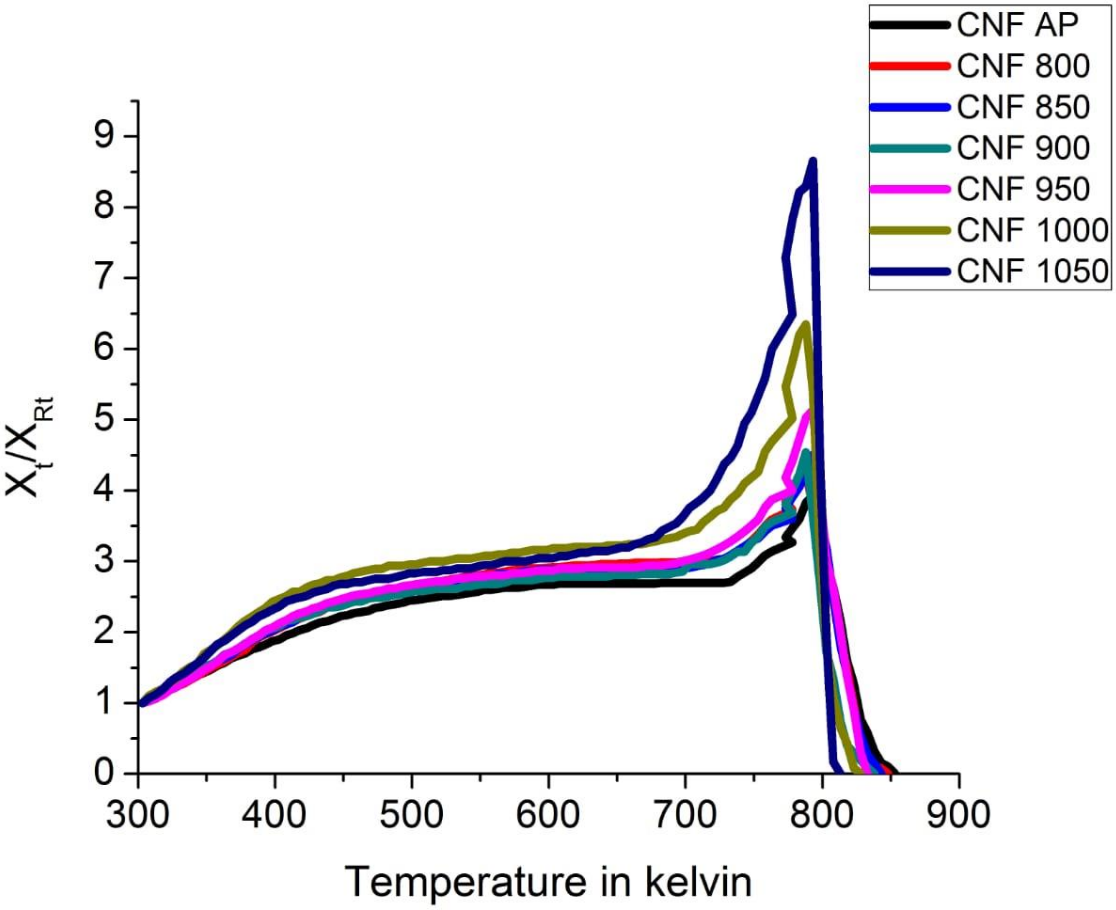

Fig. 9. The Plot of normalised AC susceptibility versus temperature of 'AS PREPARED' and 'SINTERED' $Co_{0.5}Ni_{0.5}Fe_2O_4$ ferrite

The normalized susceptibility curves of the ‘as prepared’ and ‘sintered’ $Co_{0.5}Ni_{0.5}Fe_2O_4$ ferrite are shown in Fig. 9 and the Curie temperature obtained using this plot is given in Table 6. The behaviour of the curves in response to the temperature shows the domain nature of the nanoparticles and represents the variation in Curie transition temperature, T_c. It can be observed from Fig. 9 that these ferrite samples contain single domain-multidomain type of particles.

It is observed that as the Sintering temperature increases the Tc decreases which have occurred due to the predominance of the effect due to change in cation distribution over the finite size.

Table 6: The curie temperature of $Co_{0.5}Ni_{0.5}Fe_2O_4$ ferrite samples.

Sr. No.	Sample	T_c in kelvin
1	CNF AP	853
2	CNF 800	847
3	CNF 850	842
4	CNF 900	837
5	CNF 950	831
6	CNF 1000	825
7	CNF 1050	813

CHAPTER –IV

CONCLUSION

4. Conclusion

Solid state reaction between cobalt nitrate, nickel nitrate and ferric nitrate using D-malic acid assisted combustion route maintaining ratio as 1:1.111 resulted in formation of single phase $Co_{0.5}Ni_{0.5}Fe_2O_4$ ferrite. The prepared ferrites ‘As Prepared’ as well as ‘sintered’ ferrite were characterised using XRD, FTIR and SEM techniques. The chemical analysis data of “AS PREPARED” sample which include Nickel, Cobalt, and Iron were found to be closely matching with the theoretical content. The XRD patterns confirmed the formation of single phase of “as prepared” ferrite and it was duly supported by infrared spectroscopic studies. The particle size was found to be in the range of 28 nm while the lattice parameter obtained for this ‘as prepared’ ferrite sample was 8.305Å. IR spectra of “as prepared” ferrite samples exhibit absorption bands at about $592cm^{-1}$ and $363cm^{-1}$ which are due to the metal–oxygen stretching vibrations of tetrahedral and octahedral sites, respectively. Scanning electron microscopy images revealed that as sintering temperature increases the average grain size increases which is in micron size range while ‘as prepared’ ferrites are having comparatively smaller particle size which is in nanosize range. It is observed that particles possess nearly spherical morphology. The temperature variation of DC resistivity of ‘as Prepared’ ferrite showed semiconducting behaviour. The decrease in dielectric constant with increasing frequency is a normal behaviour observed in spinel ferrites was observed for all the ferrite samples. With increase in frequency, role of grain boundaries starts decreasing, hence energy losses start decreasing. The maximum dielectric losses are obtained for composition CNF 950 in the scanned frequency range. Thermoelectric power studies displays CNF AP and CNF 800 as p-type semiconductor initially at room temperature but changes to n-type at higher temperature indicating that electrons are responsible for conduction whereas CNF 900 behaves as n-type semiconductor initially which then changes to p-type semiconductor at higher temperature indicating that holes are responsible for conduction .The normalized A.C. susceptibility plots of ferrites conclude the presence of particles with a predominantly single domain-multidomain type wherein Curie temperature decreases with increase in sintering temperature.

5. References

[1] V. ˇ Sepel´ak , D. Baabe, D. Mienert , D. Schultze, F. Krumeich, F. J. Litterst and K. D. Becker, J. Magn. Magn. Mater., 257 (2003) 377.

[2] C.V. Ramana , Y.D. Kolekar, K. K. Bharathi, B. Sinha and K. Ghosh, Journal of applied physics, 114 (2013) 183907

[3] N.M. Deraz, J. Anal. Appl. Pyrolysis, 82 (2008) 212.

[4] Z. Youcai, R. Stanforth, Miner. Eng. 13 (2000) 1417.

[5] J.H. Lee, C.K. Kim, S. Katoh, R. Murakami, J. Alloys Compd. 325 (2001) 276.

[6] W.J. Dawson, J. Am. Ceram. Soc. 67 (1988) 1673.

[7] C.K. Kim, J.H. Lee, S. Katoh, R. Murakami, M. Yoshimura, Mater. Res. Bull. 36 (2001) 2241.

[8] A. Meenakshisundaram, N. Gunasekaran, V. Srinivasan, Phys. Status Solidi A, 69 (1982) K15.

[9] V. Pallai, D.O. Shah, J.Magn. Magn. Mater. 163 (1996) 22.

[10] R. Skomski, J. Phys.: Condens. Matter, 15 (2003) R841.

[11] N.M. Deraz, M.K. El-Aiashy, S.A. Ali, Adsorpt. Sci. Technol. 27 (2009) 797.

[12] K. Maaz, W. Khalid, A. Mumtaz, S.K. Hasoianain, J. Liu, J.L. Duan, Physica E, 41 (2009) 593.

[13] M Tan , K¨oseoˇglu Y,F Alan and Sent¨urk E 2011 J. Alloys Compd., 509 9399

[14] S Patange , S E Shirsath,, G K Jangam Lohar, S S Jadhav and K Jadhav, J. Appl. Phys. 109 (2011) 053909

[15] M U Islam, T Abbas ,S B Niazi, Z Ahmad , S Sabeen and M A Chaudhry , Solid State Commun. 130 (2004) 353

[16] He X M, Yan S M, Li ZW, X Zhang ,X Y Song, W Qiao, ZhongWand Du Y W, 2015 Chin. Phys. B, 24 (2015) 127502.

[17] N.M. Deraz, A. Alarifi, Ceram. Int. 38 (2012) 4049.

[18] T. Aouak, N. Deraz, A. Alarifi, Bull. Mater. Sci. 36 (2013) 417.

[19]A Manikandan,., M Durka, S.A Antony , J. Supercond. Novel Magn. **27**(12) (2014) 2841–2857

[20] E Hema , A Manikandan,.,P Karthika,, S A Antony, , J. Supercond. Novel Magn. **28**(8), 2539–2552 (2015)

[21]S Singhal., J Singh, S Barthwal,, K Chandra, J. Solid State Chem. **178**(10) (2005) 3183–3189

[22] J.R. Liu, M. Itoh, K.I. Machida, Appl. Phys. Lett. 88 (2006) 062503.

[23] Y.L. Cheng, B.L. Zou, J.L. Yang, C.J. Wang, Y.J. Liu, X.Z. Fan, L. Zhu, Y. Wang, H.M. Ma, X.Q. Cao, Cryst. Eng. Comm., 13 (2011) 2268–2272.

[24] L.J. Song, S.W. Su, Q.F. Lu, G. Zhao, Appl. Surf. Sci., 258 (2012) 3789–3794.

[25] A. Maqsood, K. Khan, J. Alloys Compd., 509 (2011) 3393–3397.

[26] S.R. Borhade, S.B. Waghmode, Beilstein J. Org. Chem. 7, 310 (2011)

[27]. I. Sharifi, H. Shokrollahi, S. Amiri, J. Magn. Magn. Mater. 324 (2012) 903

[29] L. Yang, Y. Xie, H. Zhao, X. Wu, Y. Wang, Solid-State Electron. 49 (2005) 1029

[30] Mathew George, Swapna S Nair, K A Malini, P A Joy and M R Anantharaman, JOURNAL OF PHYSICS D: APPLIED PHYSICS· **40** (2007) 1593–1602

[31] R C Kambale, P A Shaikh, C H Bhosale, K Y Rajpure and Y D Kolekar,·Smart Mater. Struct. **18** (2009) 085014 (6pp)

[32] JunXiang, YanqiuChu, XionghuiZhang, XiangqianShen, Applied Surface Sci., 263(15)(2012) 320-325.

[33] Lei Zhang, Chunsheng Shi, Kyong Yop Rhee, Naiqin Zhao, Composites Part A: Applied Science and Manufacturing, 43(12) (2012) 2241-2248.

[34] L. R. Gonsalves,V. M. S. Verenkar, J. Therm. Anal. Calorim., 108 (2012) 877–880.

[35] N.M.Deraz, Omar H. Abd-Elkader, Journal of Industrial and Engineering Chemistry, 20(5) (2014) 3251-3255

[3**6**] Kishwar Khan[2014]Journal of Superconductivity and Novel Magnetism, Volume 27, Issue 2, pp 453–461

[37] Sara Bakhshayesh,Hossein Dehghan[2014],Journal of the Iranian Chemical Society .Volume 11, Issue 3, pp 769–780

[38] Hafiz M.I.AbdallahThomasMoyoNokw [2015],Journal of Magnetism and Magnetic Materials Volume 394, 15 November 2015, Pages 223-228.
hafiz27, pp 7105–7108.

[42] YingLinJingjingWangHaiboYangLeiWangMinjuanCao[2013] Journal of Industrial and Engineering ChemistryVolume 20, Issue 5, Pages 3251-3255.

[43] Jindi Feng ,Rui Xiong,Li Cheng,Yong Liu[2017] Journal of Superconductivity and Novel Magnetism, Volume 30, Issue 12, pp 3513–3521

[44] R. Kesavamoorthi,C. Ramachandra Raja[2017]..Journal of Superconductivity and Novel MagnetismVolume 30, Issue 9, pp 2535–2540

[45] Gangothri S. Kumar,T. Raguram,K. S. Rajni,(2019) Journal of Superconductivity and Novel Magnetism.Volume 32, Issue 6, pp 1715–1723

[46] V. M. Kanevsky,A. V. Butashin,A. E. Muslimov[2018].Journal of Surface Investigation: X-ray, Synchrotron and Neutron Techniques. Volume 12, Issue 6, pp 1155–1158.

[47] BrajeshNandan, M.C.Bhatnagar, Subhash C.Kashyap[1][2019] Journal of Physics and Chemistry of SolidsVolume 129, June 2019, Pages 298-306

[48] Mayara dos Santos Amarante[1], et al [2019] Sintering behavior and electromagnetic properties of a Ni–Co ferrite/NiO biphasic ceramic, Materials Research Express, Volume 6, Number 7

[49] D.M. Coutinho, V.M.S. Verenkar, J. Therm. Anal. Calorim. 128 (2017) 807–817

[50]L.R. Gonsalves, S.C. Mojumdar, V.M.S. Verenkar, J. Therm. Anal. Calorim. 104 (2011) 869–873,

[51] U.B. Gawas, V.M.S. Verenkar , S.R. Barma, S.S. Meena , Pramod Bhatt, Journal of Alloys and Compounds 555 (2013) 225–231

[52] Pratik A. Asogekar, V.M.S. Verenkar, Ceramics International,45(2019) 21793-21803

[53] B.L.Patil,S.R.Sawant,S.S. Suryavanshi and S.S. Patil, Bull Mater. Sci.,16 (1993) 267.

[54] Kunal Pubby, K. Vijay Babu, Sukhleen Bindra Narang, Materials Science & Engineering B , 255 (2020) 114513